RADIATIVE TRANSFER CODES APPLIED TO HYPERSPECTRAL DATA FOR THE RETRIEVAL OF SURFACE REFLECTANCE

K. Staenz and J. Secker
Canada Centre for Remote Sensing
Ottawa, Ontario, Canada K1A 0Y7
E-mail: karl.staenz@ccrs.nrcan.gc.ca

B.-C. Gao and C. Davis
Naval Research Laboratory
Washington, D.C. 20375, U.S.A.

KEY WORDS: Surface reflectance retrieval, radiative transfer codes (ATREM, CAM5S, MODTRAN4), hyperspectral data (AVIRIS, *casi*™)

ABSTRACT

The present investigation evaluates surface reflectance retrieved from Airborne Visible/Infrared Imaging Spectrometer (AVIRIS) and Compact Airborne Spectrographic Imager (*casi*™) data using the atmospheric radiative transfer (RT) codes: ATREM, CAM5S, and MODTRAN4. The retrieved surface reflectances were compared with ground-based reflectances acquired with a GER3700™ spectroradiometer for a playa and canola target. The results showed that the best overall performance was achieved with MODTRAN4, followed by ATREM and CAM5S. Major differences occur in the stronger gas absorption regions. At wavelengths unaffected by strong gaseous absorption, the performance was similar for the three RT codes even though ATREM and CAM5S have faster execution times.

1. INTRODUCTION

Surface reflectance retrieval in hyperspectral remote sensing is an important step in the data processing chain for the extraction of quantitative information in many applications areas. In order to calculate surface reflectance from remotely measured radiance, radiative transfer (RT) codes play an important role for removal of the atmospheric scattering and gaseous effects (Conel et al., 1988; Teillet et al., 1991; Gao et al., 1993; Green et al., 1996; Richter, 1996; Staenz and Williams, 1997). Given the high volume and complexity of hyperspectral data, the surface reflectance retrieval results depend strongly on the selected RT code as well as on the radiometric and spectral calibration of the sensor (Staenz et al., 1994 and 1995; Secker et al., 2000).

This study concentrates on the evaluation of the surface reflectance retrieved with the three atmospheric RT codes CAM5S (Canadian Advanced Modified 5S; O'Neill et al., 1996), ATREM (Atmospheric REMoval program; Gao et al., 1993; CIRES, 1999), and MODTRAN (MODerate atmospheric radiance and TRANsmittance model; Berk et al., 1989 and 1998). These RT codes are applied to different hyperspectral data sets acquired with the Airborne Visible/Infrared Imaging Spectrometer (AVIRIS) and the Compact Airborne Spectrographic Imager (*casi*™). The resulting surface reflectance is compared with ground-based reflectance in order to assess the accuracy of different RT code procedures. Special emphasis is given to the gaseous absorption regions where the largest errors in the retrieval of surface reflectance occur. In addition, the trade-off between the accuracy and the RT code's computation time is discussed. The main portion of the analysis was

carried out on the Imaging Spectrometer Data Analysis System (ISDAS), an advanced hyperspectral analysis software package developed at the Canada Centre for Remote Sensing (Staenz et al., 1998).

2. DATA SETS

Two hyperspectral data sets, acquired with AVIRIS and *casi*™, respectively, were used for this study. Concurrent ground reference information was collected during the AVIRIS overpass. This included ground-based reflectance data, aerosol optical depth, and water vapour content. None of these data were available for the *casi* cube.

The AVIRIS data set was collected over the Railroad Valley playa (Nevada, U.S.A) on June 17, 1998. AVIRIS acquires imagery at approximately 20 m ground resolution in 224 spectral bands, each about 10 nm wide, in the 400-nm to 2500-nm wavelength range (Vane et al., 1993). Concurrent ground information includes reflectance data acquired with a GER3700™ spectroradiometer from the playa target and solar disk measurements with a Microtops-II™ sunphotometer to derive aerosol optical depth at 550 nm and column water vapour. The playa target is located in flat terrain and covers a 100-m x 100-m homogeneous area. It is a relatively smooth surface of compacted clay-rich lacustrine deposits. Twenty measurements were averaged to derive a representative reflectance spectrum of this site. The target reflectances, derived with a Spectralon™ panel, were then corrected for the panel's reflectance and anisotropy and convolved to the AVIRIS bands. The co-location of ground and airborne data was achieved visually using road boundaries.

A *casi*™ data set acquired over an agricultural test site near Altona, Manitoba, Canada on July 25, 1996 was also used for this study. The data set was collected in 96 contiguous, 6.8 nm wide spectral bands, sampled at 5.8 nm interval (Anger et al., 1996). In this data acquisition configuration, the swath consists of 304 pixels with a spatial resolution of 4 m across and 4 m along track at a flight altitude of about 2500 m above ground level. The wavelength range was set from 458 nm to 1000 nm.

3. RADIATIVE TRANSFER CODES

The selected RT codes are common models used in hyperspectral remote sensing to retrieve surface reflectances from at-sensor radiances. The specific features of these models are summarized in the following paragraphs.

3.1 ATREM

This model as described in CIRES (1999) uses the 6S code to model the atmospheric scattering and the Malkmus narrow band model (Malkmus, 1967) and a pressure scaling approximation to calculate atmospheric transmittances of the following gases: H_2O, CO_2, O_3, NO_2, CO, CH_4, and O_2. The water vapour content is calculated on a pixel basis using a three band ratio technique in the 940 nm and 1130 nm water absorption bands. ATREM assumes a lambertian ground boundary condition and runs on a 2.5 nm wavelength grid for spectral integration purposes. It is configured for reverse mode (at-sensor radiance to surface reflectance) runs only. Version 3.1 of ATREM was used for this study.

3.2 CAM5S

CAM5S is an improved version of the semi-analytical M5S (modified version of 5S used at the Canada Centre for Remote Sensing) code (Teillet and Santer, 1991) which is based on 5S (Tanré et al., 1990). M5S includes features such as terrain elevation and sensor altitude dependency and reverse mode computation for surface reflectance retrieval. The 6S features (Vermote et al., 1994) such as non-lambertian (BRDF: bidirectional reflectance distribution function) calculations, computation of CO_2, CH_4, and NO_2 gaseous transmissions, and new aerosol model types have been incorporated into CAM5S. The spectral resolution was also improved to optionally run the code on a 2.5 nm or 10 cm^{-1} grid, respectively. A single scattering scheme is used in CAM5S. Version 1.0 was utilized for the investigation described in this paper.

3.3 MODTRAN

This code is based on LOWTRAN7 (Kneizys et al., 1988). Major features incorporated into MODTRAN over the years include an increase in spectral resolution from 20 cm^{-1} to 1 cm^{-1}, an improved multiple scattering algorithm (N-stream discrete ordinate method), and more accurate exo-atmospheric irradiance data bases (Berk et al., 1989 and 1999; Anderson et al., 1995). Recent upgrades encompass improvements in the calculation of solar and thermal scattering from clouds and aerosols and modelling of adjacency and non-lambertian effects (Berk et al., 1998 and 1999). The latest version of this code, MODTRAN4.1, was used for this study.

4. APPROACH

The procedures to remove atmospheric effects are outlined in Figure 1. ATREM was used outside of ISDAS in its original configuration as available from the University of Colorado (CIRES, 1999) while MODTRAN4 and CAM5S were run inside ISDAS as part of a look-up table (LUT) procedure. The input parameters used to run these codes are summarized in Table 1 for the various data sets.

The MODTRAN/CAM5S procedure is based on a LUT approach with tunable breakpoints as described in Staenz and Williams (1997), to reduce significantly the number of radiative RT code runs. A selected RT code was used in forward mode to generate the radiance LUTs, one for each of a 5% and 60% flat reflectance spectrum. These LUTs were produced for seven pixel locations equally spaced across the swath, including nadir and swath edges, and for single values of aerosol optical depth (horizontal visibility) and terrain elevation, and for a range of water vapour contents. The specification of these parameters and others required for input into the RT codes are listed in Table 1. None of the BRDF options available in CAM5S and MODTRAN4 were used for this study. It should be noted that a common user interface is used for the specification of the atmospheric conditions.

For the retrieval of the surface reflectance, the LUTs were adjusted only for the pixel position and water vapour content using a bi-linear interpolation routine (Press et al., 1992) since single values for the other LUT parameters were used for the entire cube. For this purpose, the water vapour content was estimated for each pixel in the scene with an iterative curve fitting technique (Staenz et al., 1997). The surface reflectance ρ was then calculated for each pixel as follows (Teillet at al., 1991; Williams et al., 1992):

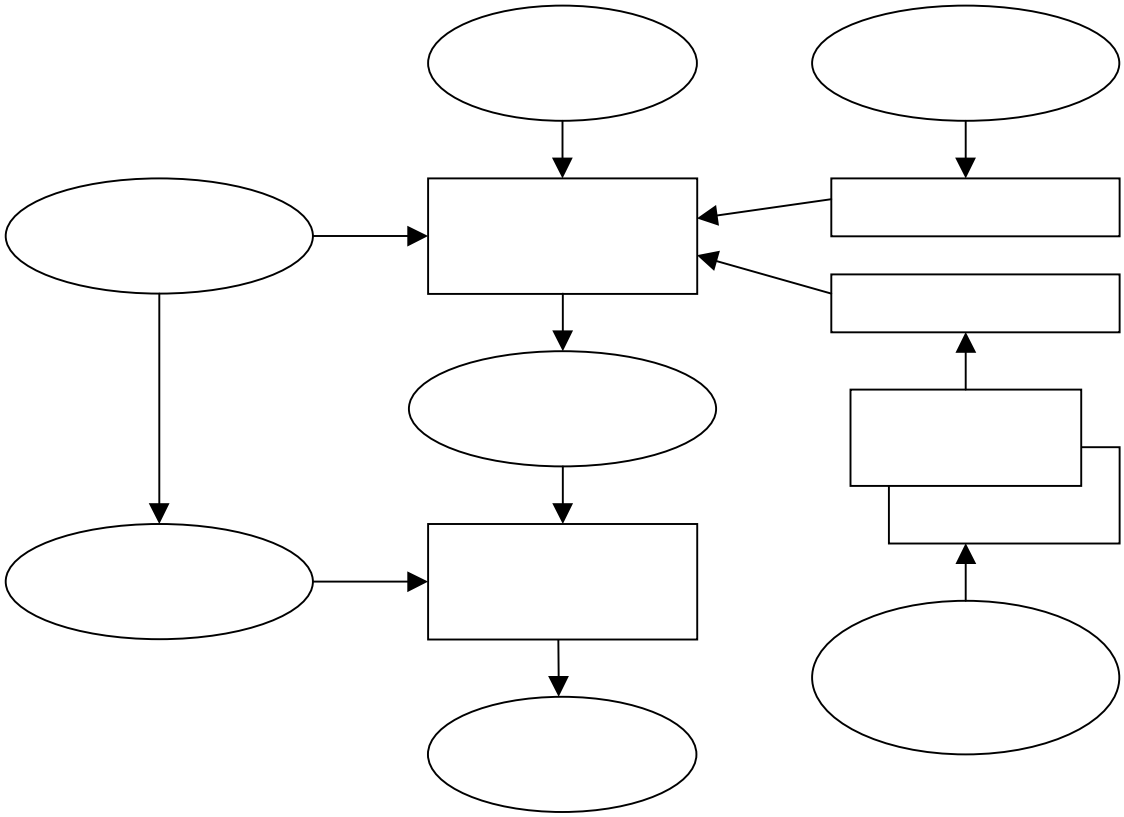

Figure 1: Processing Data Flow for the Evaluation of Surface Reflectance Retrieval with Different RT Codes (RT = radiative transfer, RSRP = relative spectral response profile, and FWHM = full width at half maximum).

$$\rho = \frac{L - L_a}{A + B + S(L - L_a)} , \tag{1}$$

where L is the at-sensor radiance provided by the image cube, L_a is the radiance backscattered by the atmosphere, S is the spherical albedo of the atmosphere, and A and B are coefficients that depend on geometric and atmospheric conditions. The unknowns A, B, S, and L_a were calculated from the equations

$$L_{gi} = A\frac{\rho_i}{1 - \rho_i S} \quad \text{and} \quad L_{pi} = B\frac{\rho_i}{1 - \rho_i S} + L_a , \tag{2}$$

where L_{gi} is the at-sensor radiance reflected by the target and L_{pi} is the at-sensor radiance scattered into the path by the atmosphere and the surrounding targets. These equations can be solved on a per pixel basis for each set of parameters $\{\rho_i , L_{gi}, \text{ and } L_{pi}\}$ obtained from the LUTs by interpolation for the different geometric and atmospheric conditions. With i = 1 and 2 (ρ_1 = 5%, ρ_2 = 60%), this yields a system of four equations with four unknowns.

Table 1: Input Parameters for Radiative Transfer Code Runs

Sensor	**AVIRIS**	***casi***™
Atmospheric model	US standard	Mid-latitude summer
Aerosol model	Continental (ATREM) Desert (CAM5S) Desert (MODTRAN4)	Continental
Date of overflight	June 17, 1998	July 25, 1996
Solar zenith angle	25.9°	31.3°
Solar azimuth angle	118.5°	155.9°
Sensor zenith angle	Fixed (ATREM) Variable (CAM5S) Variable (MODTRAN4)	Fixed (ATREM) Variable (CAM5S) Variable (MODTRAN4)
Sensor azimuth angle	Fixed (ATREM) Variable (CAM5S) Variable (MODTRAN4)	Fixed (ATREM) Variable (CAM5S) Variable (MODTRAN4)
Terrain elevation above sea level	1.435 km	0.250 km
Sensor altitude above sea level	20.800 km	2.745 km
Water vapour content	variable	variable
Ozone column	as per model	as per model
CO_2 mixing ratio	as per model (ATREM) as per model (CAM5S) 300 ppm (MODTRAN4	as per model
Aerosol optical depth @ 550 nm	0.041	--
Horizontal visibility	--	40 km

5. RESULTS

Figure 2 shows the results of the different RT code computations for the playa target from the AVIRIS scene in comparison with the reflectance acquired on the ground. The US62 (ATREM, CAM5S) and US76 (MODTRAN4) standard atmospheres in combination with the continental (ATREM) and desert aerosol models (CAM5S, MODTRAN4) were selected for the RT code runs. In this case, the measured aerosol optical depth of 0.041 was used. The code input value for the water vapour content was estimated from the image data themselves. This led to a water vapour content of 1.07 g/cm^2 (MODTRAN4), 1.49 g/cm^2 (ATREM), and 1.54 g/cm^2 (CAM5S) for the playa target. The estimated value of MODTRAN4 is close to the measured water vapour content of 1.1 g/cm^2. This means that ATREM and CAM5S overestimated the water vapour content considerably. The main reason for these differences lies most likely in the accuracy of the gaseous transmittance models and the wavelength grids selected to run these models. The finest available grids were used for the RT code runs (1 cm^{-1}: MODTRAN4, 2.5 nm: ATREM, 10 cm^{-1}: CAM5S).

a) ATREM

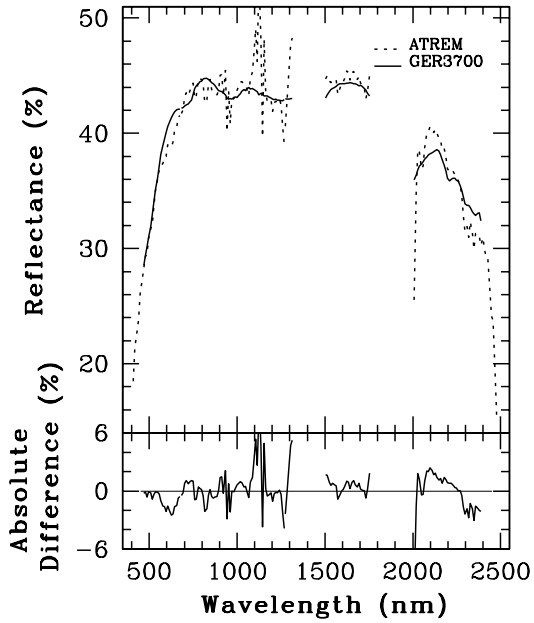

b) CAM5S

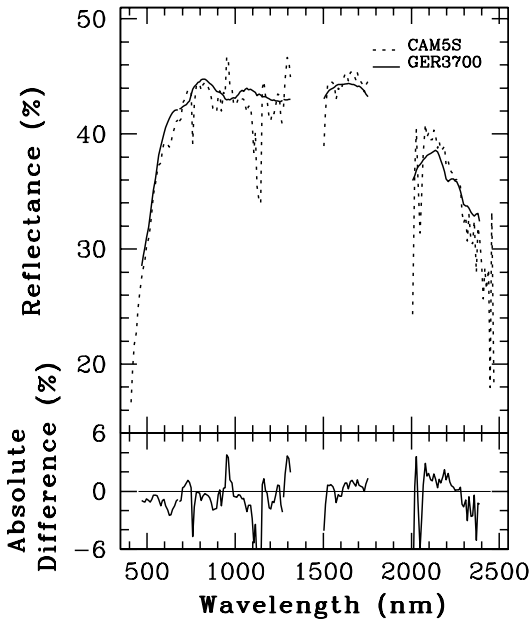

c) MODTRAN4

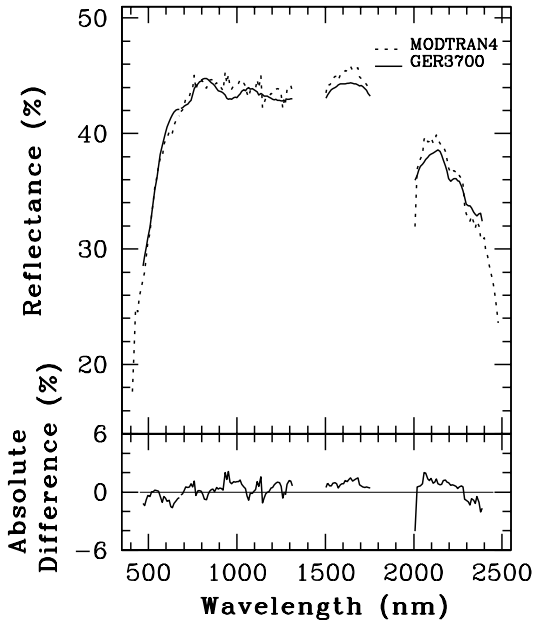

Figure 2: Comparison of Surface Reflectance Retrieved with Different RT Codes from AVIRIS Railroad Valley Playa Data with Data Measured on the Ground with a GER3700^{TM} Spectroradiometer: a) for ATREM, b) for CAM5S, and c) for MODTRAN4. The bottom plots emphasize the absolute differences between the AVIRIS and the ground spectrum. The AVIRIS spectra were averaged over a 3 x 3 pixel area while the GER3700^{TM} spectrum was generated from 20 measurements.

It is obvious from Figure 2 that the retrieved surface reflectance spectra are not as smooth as the ground-based reflectance with some exception in the visible wavelength regions. Major areas of concern are the gas absorption regions. The reflectance is especially affected in the 940-nm and the 1130-nm water absorption bands, as well as in the wings of the strong 1380-nm and 1870-nm water absorption regions. These effects would be larger for ATREM and CAM5S, if the measured water vapour content would have been used. Problems were also encountered in the O_2 absorption regions, especially in the 760-nm absorption feature for CAM5S and to some extent in the 1265-nm region for all three codes. The same is valid for the CO_2 region at 2055 nm for CAM5S and to a lesser degree for ATREM. MODTRAN4 compensated basically for this feature due to an adjustable CO_2 volume mixing ratio. This value was set to 300 ppm for this study. Although an improvement of the reflectance was achieved with this value, a mixing ratio of approximately 360 ppm is more realistic to reflect today's atmospheric CO_2 condition. The absolute difference plots show that MODTRAN4 clearly outperforms ATREM and CAM5S in the gas absorption regions. These differences are mainly due to the use of different transmittance models and wavelength grid intervals in these RT codes as pointed out in the previous paragraph. Line wing absorption effects are accounted for in the calculation of the transmittance in MODTRAN4, but not in ATREM and CAM5S.

Significant differences occur also in the 2100-nm to 2450-nm region between the retrieved and ground reflectances. These differences are mostly due to the different solar exo-atmospheric irradiance functions used in the RT codes (Staenz et al., 1995). These functions are based on Neckel and Labs (1984) and Green and Gao (1993) for ATREM, Iqbal (1983) for CAM5S, and Kurucz (1994) for the MODTRAN4 run.

MODTRAN4's performance with a maximum absolute difference of + 2 % to - 4 % between the spectral reflectance retrieved from AVIRIS data and the ground measurements is superior to the performance of ATREM (± 10 %) and CAM5S (+ 4 % to –12 %). Without consideration of the wings of the 1870-nm absorption feature, the absolute errors for the MODTRAN4 case are between ± 2%. The absolute errors translate into an average relative error between retrieved and ground-based reflectance of 2.0 % for MODTRAN4 considering the maximum absolute difference range. These relative errors become larger for ATREM (3.2 %) and CAM5S (3.7 %). The better overall performance of MODTRAN4 was expected since ATREM and CAM5S make extensive use of analytical expressions. This leads to a shorter computation time for surface reflectance retrieval using ATREM and CAM5S, approximately by a factor of 16 and 3, respectively. With each MODTRAN4 run taking 132 sec on a Sun ULTRASPARC 1 workstation, this resulted in a total computation time of 183 minutes for the AVIRIS data cube including LUT calculations, water vapour retrieval, and conversion from at-sensor radiances to surface reflectances.

Figure 3 portrays the results from the RT code runs for the canola target extracted from the *casi*™ cube. The input parameters to run the codes are summarized in Table 1. The water vapour amount was estimated on a pixel-by-pixel basis from the scene itself for the RT code computations. The results follow a similar pattern as for the AVIRIS cases with 2.84 g/cm^2 (ATREM), 2.04 g/cm^2 (CAM5S), and 1.77 g/cm^2 (MODTRAN4) for the canola site. Due to the lack of a simultaneously acquired ground-based reflectance spectrum, data collected from a canola field outside of the image cube were used as a reference. Even though the field condition was approximately the same as for the field in the *casi*™ scene, no quantitative difference measures were computed. Despite the fact that the location of the retrieved and the ground-based spectra is different, the match between the two spectra is fairly good for all three RT code runs. As for the AVIRIS cases, problems occur in the gas absorption regions, especially in the 760-nm O_2 absorption region (ATREM, CAM5S) and in the 940-nm H_2O absorption feature for all RT code cases. Without considering the large over-correction

of the reflectance in the 940-nm region, the MODTRAN4 computation achieved the best overall result. This over-correction of the reflectance for the MODTRAN4 case is not fully understood yet.

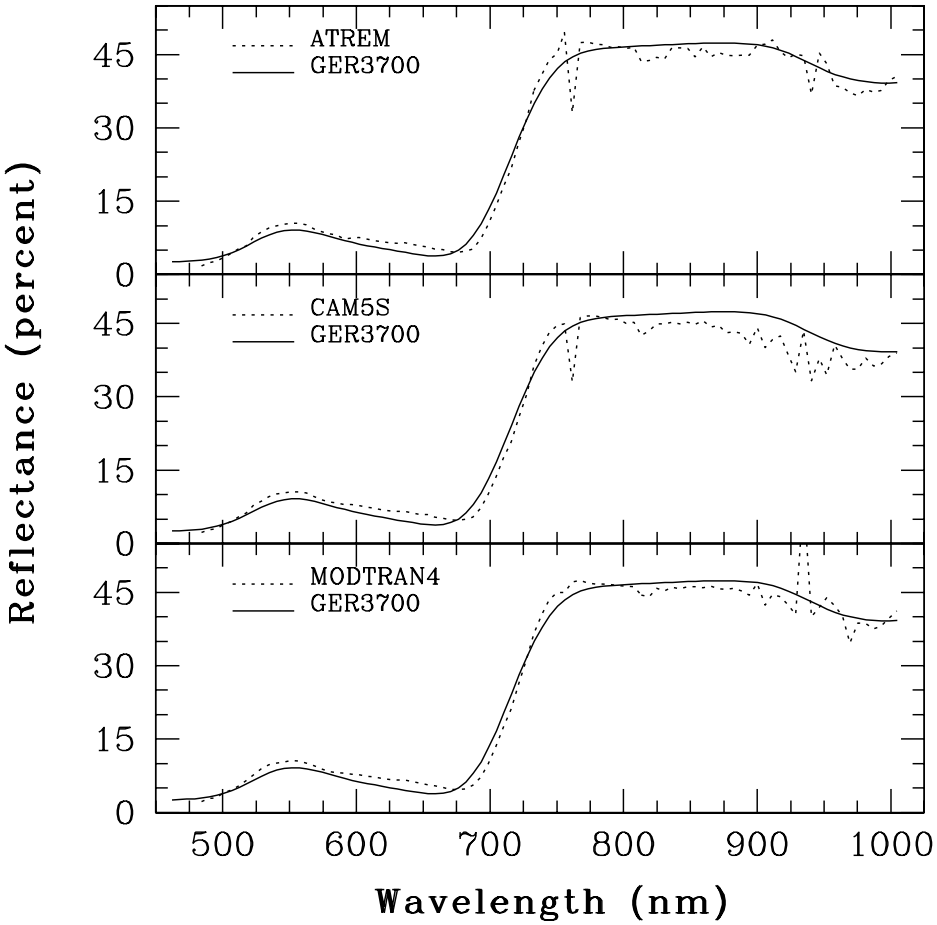

Figure 3: Canola Surface Reflectance Spectra Retrieved with ATREM (top), CAM5S (centre), and MODTRAN4 (bottom) from a *casi*™ Image Cube in Comparison with a Reflectance Spectrum Acquired on the Ground. The *casi*™ spectra were averaged over a 2 x 3 pixel area while the ground-based spectrum was retrieved from 7 measurements.

6. CONLUSIONS

Surface reflectance spectra retrieved with the RT codes ATREM, CAM5S, and MODTRAN4 from an AVIRIS data cube acquired over the Railroad Valley playa in Nevada were compared with simultaneously collected ground-based reflectances. For the ambient atmospheric condition, MODTRAN4 achieved the best results with an average relative difference of 2 %, followed by ATREM (3.2 %) and CAM5S (3.7 %). These relative differences are within the uncertainty limits of the ground-based reflectances. MODTRAN4 clearly outperformed ATREM and CAM5S in the gas absorption features, especially in the 940-nm and 1130-nm H_2O regions as well as in the 2055-nm CO_2 region. This is most likely due to the fact that MODTRAN makes use of more accurate gaseous transmittance models and a finer spectral resolution than the other two RT codes. Outside the strong gas absorption features, the performance was similar for all three RT codes with exception of the 2100-nm to 2450-nm region where differences occur mainly due the use of different exo-

atmospheric solar irradiance data bases. The results associated with the visible and near-infrared region are similar to those obtained from the *casi*™ data over the canola field. An exception is the strong over-correction of the reflectance in the 940-nm H_2O region for the MODTRAN4 run. The different RT codes used for the estimation of atmospheric water vapour from the data cubes themselves led to different water vapour values. Since ATREM and CAM5S make extensive use of analytical expressions and a coarser spectral resolution, their computation times are significantly shorter than for the MODTRAN4 runs.

7. ACKNOWLEDGEMENTS

The authors wish to thank R.P. Gauthier and G. Fedosejevs of the Canada Centre for Remote Sensing for their technical assistance and for making the AVIRIS and associated ground data over the Railroad Valley Playa available. Thanks to R. Adams and C. Nadeau of MacDonald Dettwiler and Associates Ltd. for their technical support and D.J. Williams of MacDonald Dettwiler and Associates Ltd. for implementation of CAM5S into ISDAS.

8. REFERENCES

Anderson, G.P., J. Wang, and J.H. Chetwynd, 1995. MODTRAN3: An Update and Recent Validations Against Airborne High Resolution Interferometer Measurements. Summaries of the Fifth Annual JPL Airborne Earth Science Workshop, Pasadena, California, U.S.A., JPL-Publication 95-1, Vol. 1, pp. 5-8.

Anger, C., S. Achal, T. Ivanco, S. Mah, R. Price, and J. Busler, 1996. Extended Operational Capabilities of *casi*. Proceedings of the Second International Airborne Remote Sensing Conference, San Francisco, California, U.S.A., pp. 124-133.

Berk, A., L.S. Bernstein, and D.C. Robertson, 1989. MODTRAN: A Moderate Resolution Model for LOWTRAN7. Final Report, GL-TR-0122, AFGL, Hanscom AFB, Maryland, U.S.A.

Berk, A., L.S. Bernstein, G.P. Anderson, P.K. Acharya, D.D. Robertson, J.H. Chetwynd, and S.M. Adler-Golden, 1998. MODTRAN Cloud and Multiple Scattering Upgrades with Application to AVIRIS. Remote Sensing of Environment, 65:367-375.

Berk, A., G.P. Anderson, P.K. Acharya, J.H. Chetwynd, L.S. Bernstein, E.P. Shettle, M.W. Matthew, and S.M. Adler-Golden, 1999. MODTRAN4 User's Manual. Air Force Research Laboratory, Hanscom AFB, Maryland, U.S.A.

CIRES, 1999. Atmosphere REMoval Program (ATREM), User's Guide, Version 3.1. Center for the Study from Space, Cooperative Institute for Research in Environmental Sciences (CIRES), University of Colorado, Boulder, Colorado, U.S.A.

Conel, J.E., R.O. Green, R.E. Alley, C.J. Bruegge, V. Carrère, J.S. Margolis, G. Vane, T.G. Chrien, P.N. Slater, S.F. Biggar, P.M. Teillet, R.D. Jackson, and S. Moran, 1988. In-Flight Radiometric Calibration of the Airborne Visible/Infrared Imaging Spectrometer (AVIRIS). Proceedings of the SPIE Conference on Recent Advances in Sensors, Radiometry, and Data Processing for Remote Sensing, Orlando, Florida, U.S.A., Vol. 924, pp. 197-213.

Gao, B.-C., K.B. Heidebrecht, and A.F.H. Goetz, 1993. Derivation of Scaled Surface Reflectances From AVIRIS Data. Remote Sensing of Environment, 44:165-178.

Green, R.O., and B.-C. Gao, 1993. A Proposed Update to the Solar Irradiance Spectrum Used in LOWTRAN and MODTRAN. Summaries of the Fourth Annual JPL Airborne Geoscience Workshop, Washington, D.C., JPL-Publication 93-26, Vol. 1, pp. 81 – 84.

Green, R.O., D.A. Roberts, and J.E. Conel, 1996. Characterization and Compensation of the Atmosphere for the Inversion of AVIRIS Calibrated Radiance to Apparent Surface Reflectance. Summaries of the Sixth Annual JPL Airborne Earth Science Workshop, Pasadena, California, U.S.A., JPL Publication 96-4, Vol. 135-146.

Iqbal, M., 1983. An Introduction to Solar Radiation. Academic Press, New York, New York, U.S.A.

Kneizys, F.X., E.P. Shettle, L.W. Abreu, J.H. Chetwynd, G.P. Anderson, W.O Gallery, J.E. Selby, and S.A. Clough, 1988. User's Guide to Lowtran7. AFGL-TR-88-0177, Air Force Geophysics Laboratory, Hanscom AFB, Bedford, Maryland, U.S.A.

Kurucz, R.L., 1994. The Solar Irradiance by Computation. Proceedings of the 17th Annual Review Conference on Atmospheric Transmission Models, Geophysics Directorate/Phillips Laboratory, Hanscom AFB, Maryland, U.S.A., pp.132-141.

Malkmus, W., 1967. Random Lorentz Band Model with Exponential-tailed S^{-1} Line-intensity Distribution Function. Journal of the Optical Society of America, 57: 323-329.

Neckel, H., and D. Labs, 1984. The Solar Radiation between 3300 and 12500 Angstrom. Solar Physics, 90:205-258.

O'Neill, N.T., A. Royer, and M.N. Nguyen, 1996. Canadian Advanced Modified 5S (CAM5S). Internal Report, CARTEL-1996-0202, Centre d'applications et de recherches en télédétection (CARTEL), Université de Sherbrooke, Sherbrooke, Québec, Canada.

Press, W.H., S.A. Teukolsky, W.T. Vetterling, and B.P. Flannery, 1992. Numerical Recipes in C. Cambridge University Press, Cambridge, England, pp.123-125.

Richter, R., 1996. Atmospheric Correction of DAIS Hyperspectral Image Data. Computer & Geoscience, 22(7):785-793.

Secker, J., K. Staenz, R.P. Gauthier, and B. Budkewitsch, 2000. Vicarious Calibration of Hyperspectral Sensors in Operational Environments. Submitted to Remote Sensing of Environment.

Staenz, K., D.J. Williams, G. Fedosejevs, and P.M. Teillet, 1994. Surface Reflectance Retrieval From Imaging Spectrometer Data Using Three Atmospheric Codes. Proceedings of SPIE's International Symposium on Recent Advances in Remote Sensing and Hyperspectral Remote Sensing, Rome, Italy, pp. 17-28.

Staenz, K., D.J. Williams, G. Fedosejevs, and P.M. Teillet, 1995. Impact of Differences in the Solar Irradiance Spectrum on Surface Reflectance Retrieval With Different Radiative Transfer Codes. Summaries of the Fifth Annual JPL Airborne Earth Science Workshop, Pasadena, California, U.S.A., JPL-Publication 95-1, Vol. 1, pp.153-156.

Staenz, K., and D.J. Williams, 1997. Retrieval of Surface Reflectance from Hyperspectral Data Using a Look-Up Table Approach. Canadian Journal of Remote Sensing, 23(4):354-368.

Staenz, K., T. Szeredi, R.J. Brown, H. McNairn, and R. VanAcker, 1997. Hyperspectral Information Extraction Techniques Applied to Agricultural *casi* Data for Detection of Within-Field Variations. Proceedings of the International Symposium in the Era of Radarsat and the Nineteenth Canadian Symposium on Remote Sensing, Ottawa, Ontario, Canada, 8 pages (CD-ROM).

Staenz, K., T. Szeredi, and J. Schwarz, 1998. ISDAS - A System for Processing/Analyzing Hyperspectral Data. Canadian Journal of Remote Sensing, 24(2): 99-113.

Tanré, D., C. Deroo, P. Duhaut, M. Herman, J.J. Morcrette, J. Perbos, and P.Y. Deschamps, 1990. Description of a Computer Code to Simulate the Satellite Signal in the Solar Spectrum: The 5S Code. International Journal of Remote Sensing, 11(4): 659-668.

Teillet, P.M., K. Staenz, G. Fedosejevs, 1991. A Prototype Atmospheric Correction Scheme for Airborne Imaging Spectrometer Data. Proceedings of the Fourteenth Canadian Symposium on Remote Sensing, Calgary, Alberta, Canada, pp. 127-143.

Teillet, P.M., and R. Santer, 1991. Terrain Elevation and Sensor Altitude Dependence in a Semi-Analytical Atmospheric Code. Canadian Journal of Remote Sensing, 17(1): 36-44.

Vane, G., R.O. Green, T.G. Chrien, H.T. Enmark, E.G. Hansen, and W.M. Porter, 1993. The Airborne Visible/Infrared Imaging Spectrometer (AVIRIS). Remote Sensing of Environment, 44: 127-143.

Vermote, E.D., D. Tanré, J.L. Denzé, M. Herman, and J.J. Morcrette, 1994. Second Simulation of the Satellite Signal in the Solar Spectrum (6S). 6S User's Guide, Version 0, NASA GSFC, Greenbelt, Maryland, U.S.A.

Williams, D.J., A. Royer, N.T. O'Neill, S. Achal, and G. Weale, 1992. Reflectance Extraction from CASI Spectra Using Radiative Transfer Simulations and a Rooftop Radiance Collector. Canadian Journal of Remote Sensing, 18(4): 251-261.